Journal of the European Ceramic Society 21 (2001) 2629–2632
www.elsevier.com/locate/jeurceramsoc

Structure-microwave property relations of Ca and Sr titanates

P.L. Wise[a], I.M. Reaney[a,*], W.E. Lee[a], T.J. Price[b], D.M. Iddles[b], D.S. Cannell[b]

[a]*University of Sheffield, Department of Engineering Materials, Sheffield S1 3JD, UK*
[b]*Filtronic Comtek, Four Ashes, Wolverhampton WV10 7DB, UK*

Abstract

The microwave dielectric properties of the $Sr_xCa_{1-x}TiO_3$, $Sr_{n+1}Ti_nO_{3n+1}$ and $(Sr_xCa_{1-x})_3Ti_2O_7$ series have been measured. TCF decreases from +1647 to +859 MK^{-1} as Ca content increases in the $Sr_xCa_{1-x}TiO_3$ series, due to the onset of octahedral tilt transitions. Additions of excess SrO to $SrTiO_3$ form the $Sr_{n+1}Ti_nO_{3n+1}$ series with Q a maximum for $Sr_3Ti_2O_7$. Ca substitutions to $Sr_3Ti_2O_7$ result in a solid solution limited to the Sr and Ca rich ends of the $(Sr_xCa_{1-x})_3Ti_2O_7$ series with Q a maximum of 10 250 at 2.5 GHz for $Sr_{2.4}Ca_{0.6}Ti_2O_7$ and TCF a minimum +50 MK^{-1} for $Ca_3Ti_2O_7$. The variation of TCF for the $(Sr_xCa_{1-x})_3Ti_2O_7$ series was also attributed to the onset of octahedral tilt transitions. © 2001 Published by Elsevier Science Ltd. All rights reserved.

Keywords: Alkaline earth oxides; Dielectric properties; Electron microscopy; Perovskites; X-ray methods

1. Introduction

Commercial microwave dielectrics with dielectric constants (ε_r) from 30 to 45, quality factors (Q) > 20 000 at 1 GHz and temperature coefficients of dielectric constant (TCF) $\pm MK^{-1}$ are currently fabricated from perovskite-structured Ca and Sr titanate doped with lanthanide aluminates. However, little attention has been paid to the properties of the $Sr_xCa_{1-x}TiO_3$ solid solution and even less to the effect of AO (SrO/CaO) excess.

The following sequence of transitions has recently been suggested for $Sr_xCa_{1-x}TiO_3$: Pm $\bar{3}$ m $1 \geqslant x \geqslant 0.95$–0.92, 14/mcm $0.92 \geqslant x \geqslant 0.65$, Bmmb $0.6 \geqslant x \geqslant 0.45$ and Pbnm $x < 0.4$.[1,2] The order parameter for these phase transitions is the amplitude of rotation (tilting) of the oxygen octahedra and the symmetries of the crystal structures can be predicted according to Glazer.[3]

Additions of excess SrO to $SrTiO_3$ form a homologous series with the general formula $Sr_{n+1}Ti_nO_{3n+1}$ (n indicates the number of layers of $SrTiO_3$) and are known as Ruddlesden-Popper (RP) phases.[4,5] RP phases consist of SrO layers, which separate and shear by 1/2[111] $SrTiO_3$ perovskite blocks. The phases Sr_2TiO_4, $Sr_3Ti_2O_7$ and $Sr_4Ti_3O_{10}$ have been reported, but the latter requires long heat treatments at high temperatures to form a single phase.[6] $Sr_5Ti_4O_{13}$ has not been observed experimentally. Ceh and Kolar[7] observed that excess CaO additions to $CaTiO_3$ also formed a homologous series with the general formula $Ca_{n+1}Ti_nO_{3n+1}$. The $Ca_3Ti_2O_7$ and $Ca_4Ti_3O_{10}$ compounds have been reported, but Elcombe et al.[8] demonstrated that the Ca_2TiO_4 phase could not form.

Tolerance factor (t), given by Eq. (1) where R_A, R_B, and R_O are the radii of the A-, B-site and O^{-2}-ions, respectively, is a measure of the stability of the perovskite phase,

$$t = (R_A + R_O)/\sqrt{2}(R_B + R_O) \tag{1}$$

Compounds with $t > 0.98$ are untilted whereas compounds with $t < 0.98$ have undergone at least one octahedral tilt transition on cooling.[9] Sr based RP phases are tetragonal whereas the Ca analogues are orthorhombic. The orthorhombic distortion arises because of an octahedral tilt transition driven by the low t of the perovskite blocks. Reaney et al.[9] demonstrated the relationship of t with temperature coefficient of dielectric constant, TCε, (TCε = −2(TCF + α_L) for Sr and Ba based complex perovskites. Decreasing t from 1.01 to 0.98 in complex perovskites will induce octahedral tilt transitions and force TCF/TCε towards zero, an important industrial criterion for a dielectric resonator.

The aim of this paper is to relate the microwave dielectric properties of the $Sr_xCa_{1-x}TiO_3$, $Sr_{n+1}Ti_nO_{3n+1}$ and $(Sr_xCa_{1-x})_3Ti_2O_7$ series to changes in crystal

---

* Corresponding author. Tel.: +44-114-222-5990; fax: +44-114-222-5471.
E-mail address: i.m.reaney@sheffield.ac.uk (I.M. Reaney).

PII: S0955-2219(01)00328-4

structure determined using X-ray diffraction (XRD) and transmission electron microscopy (TEM).

2. Experimental

High purity (>99.95%) $SrCO_3$, $CaCO_3$ and TiO_2 powders were processed using the conventional mixed oxide route so as to form compounds in the $Sr_xCa_{1-x}TiO_3$, $Sr_{n+1}Ti_nO_{3n+1}$ and $(Sr_xCa_{1-x})_3Ti_2O_7$ series. Starting mixtures were wet milled for 16 h, calcined (double calcined for higher Ca content) for 4 h at 1150–1350 °C in air and re-milled in propan-2-ol with 2 wt.% PEG binder. Pellets (20 mm diameter) were uniaxially pressed at 110 MPa into discs and sintered for 4 h at various temperatures in air until the highest density was achieved. A Philips X-ray diffractometer was used to characterise the phases formed and a Jeol 3010 TEM was used to verify the phase assemblage of each sample and examine the stacking sequences of these compounds. Microwave measurements were performed using an aluminium cavity ~4 times the diameter of the test resonator, (this ensured an "isolated" but shielded resonator) and a vector network analyser operating in the $TE_{01\delta}$ resonance mode in reflectance.

Table 1
Structures in the $Sr_xCa_{1-x}TiO_3$, $Sr_{n+1}Ti_nO_{3n+1}$, and $(Sr_xCa_{1-x})_3Ti_2O_7$ series determined using XRD

Composition	Structure
$SrTiO_3$	Pm $\bar{3}$ m
$Sr_{0.8}Ca_{0.2}TiO_3$	I4/mcm
$Sr_{0.5}Ca_{0.5}TiO_3$	Bmmb/Pbnm
$Sr_{0.4}Ca_{0.6}TiO_3$-$CaTiO_3$	Pbnm
"$Sr_4Ti_3O_{10}$" & "$Sr_5Ti_4O_{13}$"	Disordered RP
Sr_2TiO_4	I4/mmm
$Sr_3Ti_2O_7$-$Sr_{2.4}Ca_{0.6}Ti_2O_7$	I4/mmm
$Sr_{1.8}Ca_{1.2}Ti_2O_7$-$Sr_{0.9}Ca_{2.1}Ti_2O_7$	RP + P[a] + CaO
$Sr_{0.6}Ca_{2.4}Ti_2O_7$-$Ca_3Ti_2O_7$	$Ccm2_1$

[a] P = perovskite.

3. Results and discussion

3.1. X-ray diffraction

Table 1 summarises the phases identified in the $Sr_xCa_{1-x}TiO_3$, $Sr_{n+1}Ti_nO_{3n+1}$ and $(Sr_xCa_{1-x})_3Ti_2O_7$ series by XRD. The traces for the $Sr_xCa_{1-x}TiO_3$, $Sr_{n+1}Ti_nO_{3n+1}$ and $(Sr_xCa_{1-x})_3Ti_2O_7$ series are presented in an accompanying paper.[10] For $Sr_xCa_{1-x}TiO_3$, compositions with $x = 0.5$ are close to the Bmmb/Pbnm transition observed by Ball et al.,[1] and hence could be indexed as either phase. Single phase homologues of $Sr_{n+1}Ti_nO_{3n+1}$

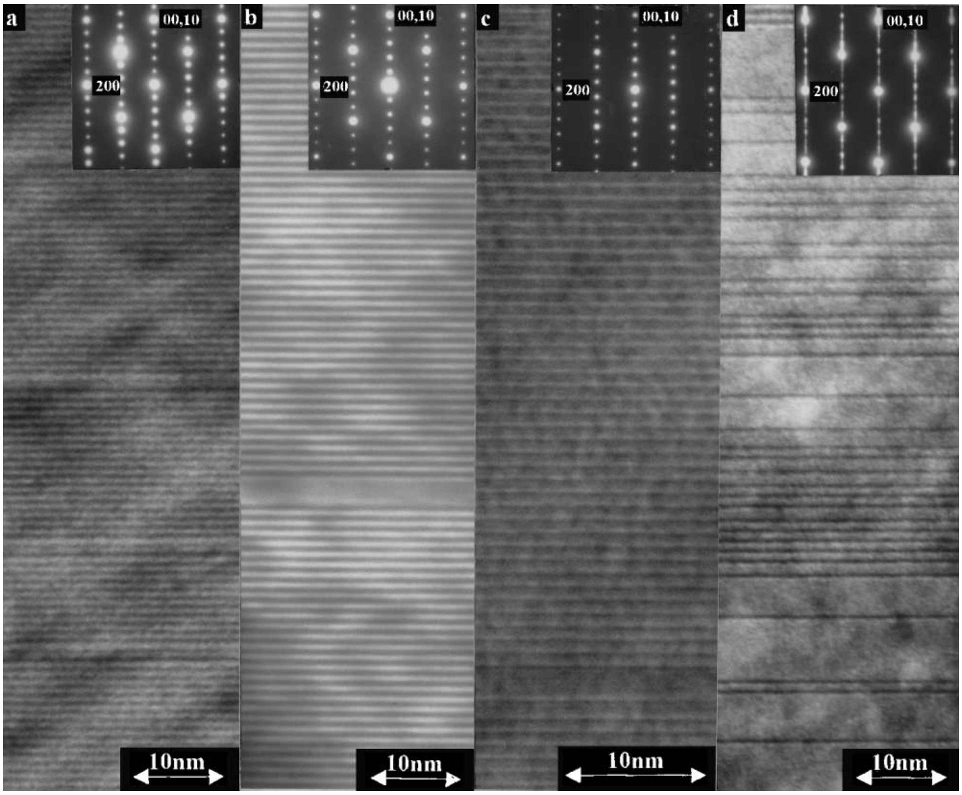

Fig. 1. (a,b,c,d). DF—TEM lattice images of $Sr_3Ti_2O_7$, $Sr_{2.4}Ca_{0.6}Ti_2O_7$, $Ca_3Ti_2O_7$ and "$Sr_4Ti_3O_{10}$" (containing slabs of various homologue phases) respectively.

were formed for $n=1$, 2 and ∞, but $n=3$ and 4 compositions were multiphase consisting of $n=1$, 2, 3 and ∞ phases.[10] Subsequently, $n=3$ and 4 are considered as disordered phases with successively decreasing excess SrO contents and are referred to as "$Sr_4Ti_3O_{10}$" and "$Sr_5Ti_4O_{13}$" respectively. Members of the $(Sr_xCa_{1-x})_3Ti_2O_7$ series with $0.6 \geqslant x \geqslant 0.3$ were found to contain perovskite, CaO and RP phases. The solubility limits for $(Sr_xCa_{1-x})_3Ti_2O_7$ were between $1 \leqslant x \leqslant 0.8$ and $0.2 \leqslant x \leqslant 0$.

3.2. Transmission electron microscopy

Fig. 1a–d shows Dark Field (DF) TEM images of selected compositions from the $(Sr_xCa_{1-x})_3Ti_2O_7$ and $Sr_{n+1}Ti_nO_{3n+1}$ series obtained with the electron beam parallel to the tetragonal or pseudotetragonal [100]/[010] direction. The stacking sequences of the perovskite (bright contrast) and rocksalt (dark contrast) layers are revealed.

$Sr_3Ti_2O_7$, $Sr_{2.4}Ca_{0.6}Ti_2O_7$ and $Ca_3Ti_2O_7$ (Fig. 1a and c) exhibit some faults from higher order RP members, which break the $n=2$ stacking sequence. "$Sr_4Ti_3O_{10}$" (Fig. 1d) demonstrates a large degree of one-dimensional disorder, compared to other RP phases, and consists of slabs (regions) of different homologue phases. The major reflections of the inserted selected area diffraction (SAD) pattern (Fig. 1d) index as the more energetically favourable $Sr_3Ti_2O_7$.[11] However, streaking indicates a mixture of homologue phases in agreement with XRD. The inset of Fig. 1c is a pseudotetragonal [110] diffraction pattern from $Ca_3Ti_2O_7$. Superlattice reflections are present which arise from rotations of octahedra around the [001] axis, associated with the orthorhombic distortion.[9]

3.3. Microwave dielectric properties

Table 2 shows Q, ε_r and TCF for the $Sr_xCa_{1-x}TiO_3$, $Sr_{n+1}Ti_nO_{3n+1}$, and $(Sr_xCa_{1-x})_3Ti_2O_7$ series, where f_o is the resonant frequency. The converted TCε data of the single phase members of the $Sr_xCa_{1-x}TiO_3$ and $(Sr_xCa_{1-x})_3Ti_2O_7$ series are compared with the t curve of Reaney et al.[9] in Fig. 2. The change in TCε for $Sr_xCa_{(1-x)}TiO_3$ occurs at the same range of tolerance factor as that for Sr and Ba based complex perovskites. Although it is tempting to suggest that octahedral tilting is responsible for tuning TCε, accompanying the onset of the structural phase transitions as Ca concentration increases, is a decrease in ε_r from 290 to 162. The Sr and Ba based compositions discudssed by Reaney et al.[9] all have ε_r between ~25 and 35. However, for $(Sr_xCa_{(1-x)})_3Ti_2O_7$ there is only a small change in ε_r from 58 to 46 and the values are closer to those for Sr and Ba based complex perovskites. In this case, it is much more likely that octahedral rotations which occur when x is near to zero, e.g. $Ca_3Ti_2O_7$, play a major role in tuning TCε/TCK.

For $Sr_{n+1}Ti_nO_{3n+1}$, there is no structural phase transition involving rotations of the octahedra since the t of the perovskite blocks remains the same throughout the

Table 2
Microwave dielectric properties of the $Sr_{n+1}Ti_nO_{3n+1}$ series

	Q	fo/GHz	ε_r	TCF/MK^{-1}
$Sr_xCa_{1-x}TiO_3$				
$SrTiO_3$[a]	2460	1.22	290	1647
$x=0.8$	2446	1.62	255	1534
$x=0.5$	3300	1.25	236	1234
$x=0.4$	5700	1.26	218	1164
$x=0.2$	6100	1.36	181	991
$x=0.1$	5900	1.41	170	931
$x=0$	8700	1.49	162	859
$Sr_{n+1}Ti_nO_{3n+1}$				
$n=1$	2616	3.14	37.4	137
$Sr_3Ti_2O_7$[b]	7450	2.53	57.9	317
"$n=3$"	5700	2.23	76.1	576
"$n=4$"	2030	1.95	99.8	801
$(Sr_xCa_{1-x})_3Ti_2O_7$				
$x=0.8$	10250	2.51	58	359
$x=0.2$	1070	2.46	60	232
$x=0.1$	1197	2.52	56	141
$x=0$	970	2.69	46	50

[a] $SrTiO_3$ is also the $n=\infty$ member of $Sr_{n+1}Ti_nO_{3n+1}$.

[b] $Sr_3Ti_2O_7$ is also the $x=1$ member of $(Sr_xCa_{1-x})_3Ti_2O_7$.

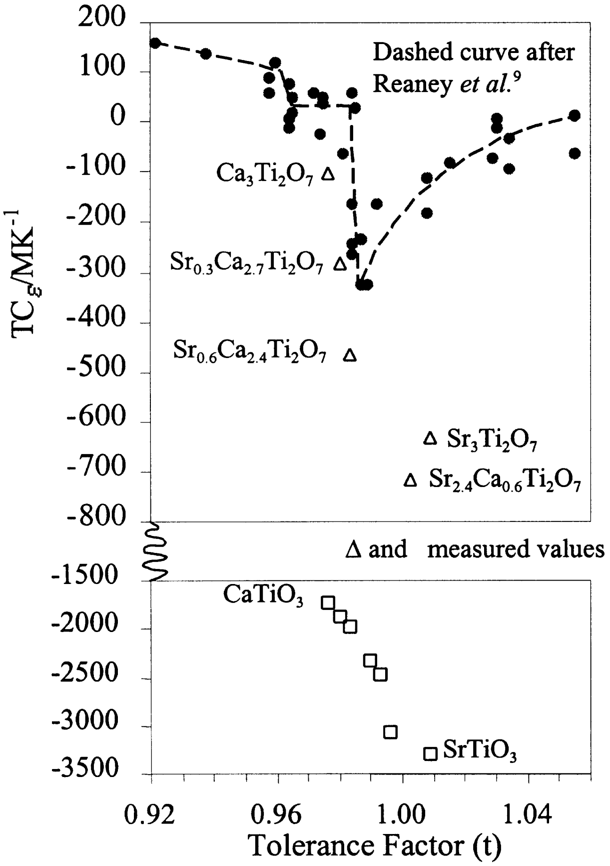

Fig. 2. TCε vs t for Sr and Ba based complex perovskites of Reaney et al.,[9] $Sr_xCa_{1-x}TiO_3$ and $Sr_xCa_{3-x}Ti_2O_7$ series.

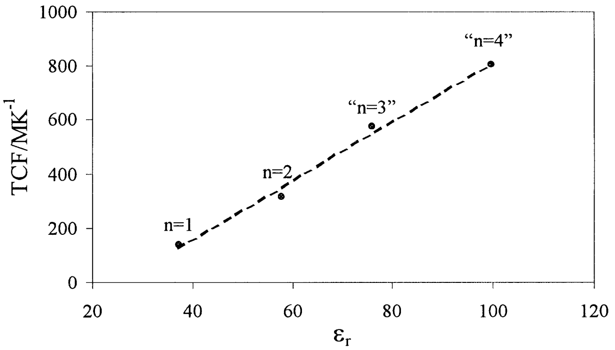

Fig. 3. TCF vs ε_r for the series $Sr_{n+1}Ti_nO_{3n+1}$.

series. Any systematic change in TCF must, therefore, arise from a mechanism other than tilting. Fig. 3 shows a plot of TCF versus ε_r (Fig. 3) for the $Sr_{n+1}Ti_nO_{3n+1}$ series (including disordered "$n=3$" and "$n=4$"); a linear relationship is observed, implying that TCF diminishes as the average ionic polarisability in the system diminishes. The dilution of polarisability can be attributed to an increase in the SrO:$SrTiO_3$ ratio as n decreases.

The values of Q throughout all the series are more difficult to interpret than TCF/TCε and ε_r. There are few systematic changes but Sr rich compositions where $n=2$ seem to show highest values. This phase has been shown by ab initio calculation to be energetically the most stable.[11]

4. Conclusion

Changes in TCF/TCε in $(Sr_xCa_{1-x})_3Ti_2O_7$ can be attributed to the onset of octahedral tilt transitions induced by decreasing tolerance factor. For the $Sr_{n+1}Ti_nO_{3n+1}$ and $Sr_xCa_{1-x}TiO_3$ series, TCF is linearly proportional to ε_r, implying that dilution of the average ionic polarisability is the mechanism for tuning TCF. The largest Q values were reported for Sr rich members of $(Sr_xCa_{1-x})_3Ti_2O_7$ with $x=1$ (7450 at 2.5 GHz) and 0.8 (10 250 at 2.5 GHz).

References

1. Ball, C. J., Begg, B. D., Cookson, D. J., Thorogood, G. J. and Vance, E. R., Structures in the system $CaTiO_3/SrTiO_3$. *J. Solid State Chem.*, 1998, **139**, 238–247.
2. Qin, S., Becerro, A. I., Seifert, F., Gottsmann, J. and Jiang, J., Phase transitions in $Ca_{1-x}Sr_xTiO_3$ perovskites: effects of composition and temperature. *J. Mater. Chem.*, 2000, **10**, 1609–1615.
3. Glazer, A. M., The classification of tilted octahedra in perovskites. *Acta. Cryst. B*, 1972, **28**, 3384.
4. Ruddlesden, S. N. and Popper, P., New compounds of the K_2NiF_2 type. *Acta. Cryst.*, 1957, **10**, 538–539.
5. Ruddlesden, S. N. and Popper, P., The compound $Sr_3Ti_2O_7$ and its structure. *Acta. Cryst.*, 1958, **11**, 54–55.
6. Hawkins, K. D. and White, T. J., Defect structure and chemistry of $(Ca_xSr_{1-x})_{n-1}Ti_nO_{3n+1}$ layer perovskites. *Phil. Trans. R. Soc. Lond. A*, 1991, **336**, 541–569.
7. Ceh, M. and Kolar, D., Solubility of CaO in $CaTiO_3$. *J. Mater. Sci.*, 1994, **29**, 6195–6300.
8. Elcombe, M. M., Kisi, E. H., Hawkins, K. D., White, T. J., Goodman, P. and Matheson, S., Structure determinations for $Ca_3Ti_2O_7$, $Ca_4Ti_3O_{10}$, $Ca_{3.6}Sr_{0.4}Ti_3O_{10}$ and a refinement of $Sr_3Ti_2O_7$. *Acta. Cryst.*, 1991, **B47**, 305–314.
9. Reaney, I. M., Colla, E. L. and Setter, N., Dielectric and structural characteristics of Ba-based and Sr-based complex perovskites as a function of tolerance factor. *Jpn. J. Appl. Phys.*, 1994, **33**, 3984–3990.
10. Wise, P. L., Reaney, I. M., Lee, W. E., Price, T. J., Iddles, D. M. and Cannell, D. S., Structure-microwave property relations in $(Sr_xCa_{(1-x)})_{n+1}Ti_nO_{3n+1}$. To be published in *J. Eur. Ceram. Soc.* Conference Proceedings from Electroceramics VII, Portoroz, Slovenia, 2000.
11. Udayakumar, K. R. and Cormack, A. N., Non-stoichiometry in alkaline-earth excess alkaline-earth titanates. *J. Phys. Chem. Solids*, 1989, **50**, 55–60.